High-pressure STM studies of oxidation catalysis

Bobaru, Ş.C.

Chapter 5

CO oxidation on Pt(111):overlayers, oxidation and reaction oscillations

In this Chapter we describe in-situ STM observation of Pt(111) during the catalytic oxidation of CO at atmospheric pressure (1.25) bar and elevated temperatures. Similar to the palladium surfaces of Chapter 3 we observe the presence of two reaction branches, one corresponding to a metallic surface and the other to a surface oxide. Oscillations between these two branches are also observed.

5.1 Introduction

As explained in the introductory chapter the most important three criteria that need to be met before a metal can be regarded as a "good" catalyst for any reaction are: good selectivity for the specific reaction, high activity for that reaction and long active life. Platinum based catalysts have many applications. We mention here the catalytic combustion of hydrocarbons and CO, in the treatment of vehicle exhaust gases and in the purification of hydrogen for use in fuel cells. Platinum is also a good catalyst for the production sulphuric acid and for the production of nitric acid via NH_3 oxidation to NO_2. Another application is the conversion of alcohol to formaldehyde [1]. Moreover platinum is a catalyst in the production of biodegradable elements for household detergents [2]. It is also one of the most used materials in electrocatalysis.

In Chapter 2 and 3 we already mentioned that self-sustained oscillations in reaction rate have been observed during CO oxidation over platinum crystals [3], similar to those on palladium surfaces. Interestingly, in previous work by our group on Pt(110) no reaction oscillations have been observed. In this chapter we turn to the (111) surface of Pt. We will see that, similar to Pt(110) and the Pd surfaces investigated in the previous chapter, the Pt(111) surface is oxidized at sufficiently high oxygen pressures. Again we observe the existence of two distinct reaction branches. By contrast with Pt(110) we do observe reaction oscillations on Pt(111). We will discuss the similarities and differences in structure, reactivity and oscillation behaviour with the other Pd and Pt surfaces. We will start this chapter with a brief description of Pt(111) and with summaries of previous work on platinum oxides and on the interaction of Pt with CO at high pressures.

5.2 Structure of clean Pt(111)

The crystal structure of platinum is face-centred cubic with a lattice parameter at 20°C of 0.392 nm. Among the low-index surfaces of platinum, the (111) plane is preferred by the majority of the researchers, due to its flatness and its low surface energy. Atoms in the (111) plane have 9 nearest neighbours, which should be compared with their regular coordination number of 12 in the bulk. Pt(111) surface has a step height of 2.2 Å. Figure 5.1 shows a ball model of this unreconstructed, close-packed surface.

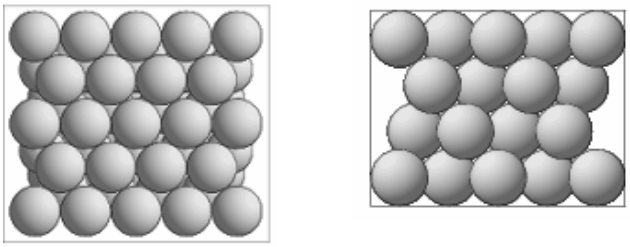

Figure 5.1: *Plan and profile views of (111) of platinum surface using a hard-sphere model.*

5.3 Previous work on Pt(111)

5.3.1 Existence and stability of surface platinum oxides - a literature survey

Since platinum is one of the elements that are well known for their chemical inertness to oxidation, the existence and stability of surface platinum oxides have been extensively studied for a long time. Nevertheless, the structures and properties of the surface platinum oxides have been poorly characterized and sometimes their existence has even been questioned. In an early study Moore and Pauling reported that PtO is probably isostructural with PdO and PtS [3]. Galloni and Roffo have used X-ray diffraction to find a body-centered cubic lattice for Pt_3O_4 [4]. Reinterpreting these diffraction data, however, Shishakov et al. have concluded that the actual composition of this oxide was not Pt_3O_4, but Pt_3O_8 [5]. In the work by Ariya et al., Pt_3O_4 has been described as a tetragonal lattice with unit cell dimensions of $a_o = 7.98$ Å and $c_o = 5.44$ Å [6]. The hexagonal structure of PtO_2 has been determined by Busch et al. [7]. According to these authors, at low temperatures only an amorphous oxide is formed. Only after a heat treatment at 350ºC the hexagonal lattice was visible. In 1968 Müller and Roy have investigated the Pt-O system using X-ray powder diffraction at high oxygen pressures (up to 3.500 bar) and temperatures ranging from

400ºC to nearly 900ºC. They identified three platinum oxide phases: the hexagonal α-PtO_2 with $a_o = 3.10$ Å and $c_o = 4.8$ Å, a new phase β-PtO_2 ($CaCl_2$ structure) with $a_o = 4.486$ Å, $b_o = 4.537$ Å, $c_o = 3.138$ Å, and Pt_3O_4 [8].

Using the tools of surface science the formation of platinum oxides on low-index surfaces of single-crystalline platinum and on polycrystalline platinum has been studied under conditions ranging from UHV to ambient pressures. Berry has studied the multilayer surface oxidation of polycrystalline Pt wire using a high-precision electrical resistance technique. His observations have shown that the oxide growth commences within 3 h after the Pt is exposed to about 1 bar of O_2 at 450ºC; once started, the oxide growth will continue at temperatures in the range of 450-560ºC [9]. From their Auger electron spectroscopy studies of the oxidation of Pt(111) Bonzel and co-workers have concluded that not platinum, but oxidized Si impurities are responsible for structures that would have been mistaken for a surface "platinum oxide" [10]. In an extensive study Salmeron *et al.* have used LEED to identify the oxide structure formed on Pt(111), Pt(332) and Pt(110) under UHV conditions. All structures found could be related to hexagonal planes of PtO_2 [11]. Studying the oscillatory CO oxidation on a supported catalyst, EuroPt-1, at atmospheric pressure, Hartmann and co-workers found the existence of a mixture of PtO and Pt_3O_4 [12].

5.3.2. Interaction of Pt(111) with CO

The adsorption system carbon monoxide on Pt(111) is without any doubt one of the "Drosophilae" of surface science and a large database on this interaction has been acquired under UHV conditions. Trying to bridge the so-called "pressure gap", several research groups have recently extended these studies to intermediate and high pressures.

Structural and energetic information about the adsorbed CO layer in equilibrium with the gas phase has been obtained using a variety of techniques. From LEED investigations under UHV conditions Ertl and co-workers have concluded that the heat of adsorption of CO on Pt(111) is strongly coverage dependent [13]. A ($\sqrt{3}$x$\sqrt{3}$)-R30º pattern was identified up to θ_{CO}=1/3, which transformed into a c(4x2) structure at θ_{CO}=1/2. As a saturation value of θ_{CO}=0.68 was approached a hexagonal close-packed CO layer was formed. The atomic resolution introduced by the STM has enabled the imaging of the CO overlayer structures, also under ambient conditions, which has initiated a debate about the inequivalence between the structures found in vacuum and under atmospheric pressures. Jensen and collaborators [14] have investigated a stepped and a flat Pt(111) surface in a CO-rich atmosphere at room temperature. At pressures higher than 200 torr a hexagonal, close-packed layer of CO was identified. The layer is incommensurate with the Pt(111) substrate, showing an intermolecular

separation of 3.7 Å and a Moiré pattern with a period of 12 ± 1 Å. According to Jensen et al., no ordered CO structure was observed at pressures lower than 1×10^{-4} bar. Kruse Vestergaard et al. investigated Pt(111) under 1 bar of CO at room temperature. These authors found two rotational domains of a hexagonal Moiré pattern with a period of 11.8 ± 0.4 Å, rotated over $24 \pm 2°$ with respect to the structure of the underlying Pt substrate [15]. The unit cell of this new structure was identified as (√19x√19) R23.4°-13CO. At low pressures (10^{-6} Torr) and low temperatures (170 K) the same Moiré pattern was observed. Based on their measurements Kruse Vestergaard et al. have concluded that increasing the pressure is equivalent with decreasing the temperature, which is to be expected on the basis of thermodynamics, provided that the kinetic barriers can be overcome at the lower temperature so that equilibrium is established on an acceptable timescale. The results in Ref. [15] are in good agreement with earlier low-temperature LEED studies and "in situ" electrochemical studies (STM combined with IRAS) [16].

5.4. Experimental

The experiments presented in this paper have been performed using the home-built combined flow Reactor-STM described in detail in the introductory chapter. This combination allows us to image the surface of a model catalyst during a reaction at atmospheric pressures. Simultaneously, we can determine the catalytic activity by analysis of the gas flow leaving the reactor using a quadruple mass spectrometer. Connected to the Reactor-STM we have a dedicated gas system especially made for high-pressure use, which allows us to independently mix the high purity gases in the desired ratios, set the pressure in the reactor and control the flow rate.

The Pt single-crystal (Czochralski grown, 5N purity) was purchased from Surface Preparation Laboratory [17], where it was spark eroded to a cylindrical shape with a diameter of 10 mm and a thickness of 2 mm and where its surface was mechanically polished to within 0.1° from the (111) orientation. In our UHV system, the surface was further prepared by repeated cycles of Ar^+ ion sputtering and O_2 (1×10^{-6}mbar) treatment at 800-900 K, followed by annealing in UHV at ~1100 K. The cleanliness and crystalline order of the surface has been checked with LEED and with the STM.

5.5 Results and discussion

5.5.1 CO adsorption on Pt(111) at ambient pressure

Images A and B in Figure 5.2 have been recorded in 1 bar of CO at room temperature. They show the Moiré pattern, previously identified by Kruse

Vestergaard et al. [15]. After this observation, we heated the sample for 2 hours to 393 K in a 1.18 bar flow of CO (the partial pressure of O_2 has been low 4.6×10^{-4} mbar). Image C was recorded under these conditions. Even though the resolution in image C is not as good as that in images A and B (due to the thermal drift the Moiré pattern seems stretched) the (√19×√19) R23.4°-13CO overlayer can be recognized.

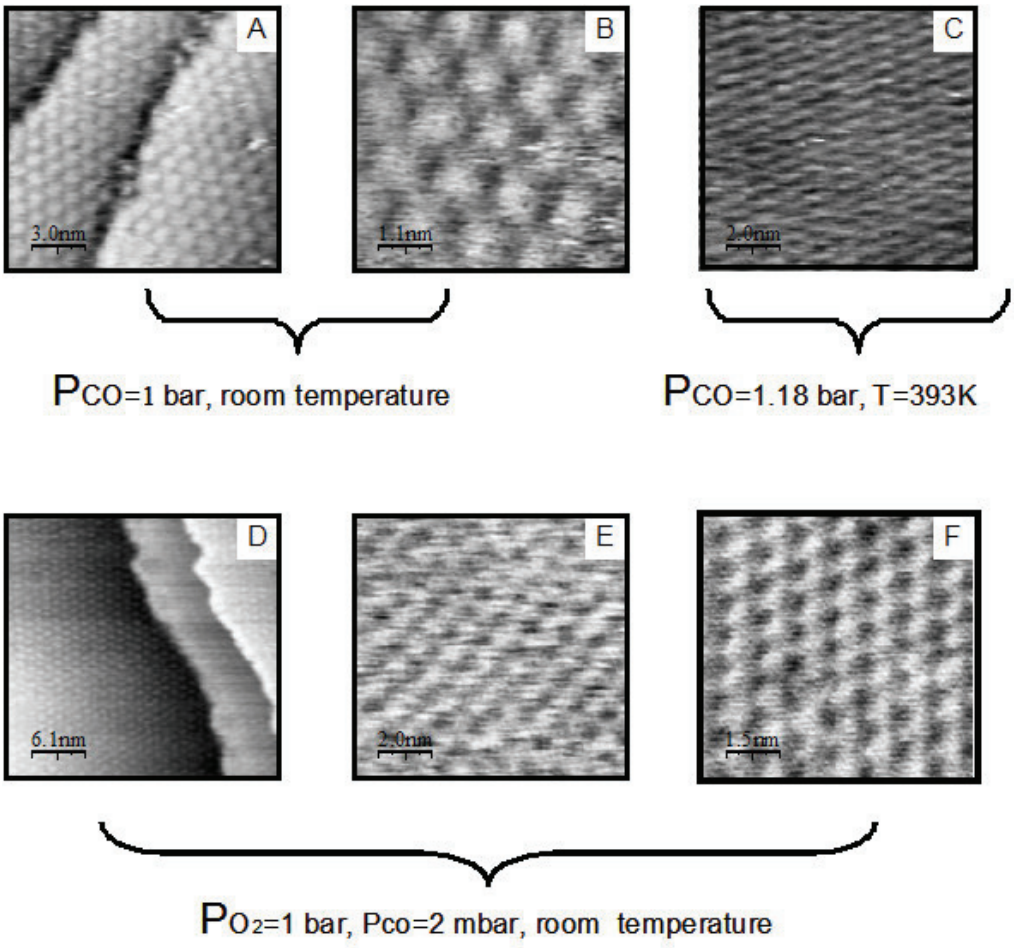

Figure 5.2: *STM images illustrating the formation and stability of the Moiré pattern of a dense, (√19×√19) R23.4°-13CO overlayer of CO molecules on Pt(111) under different gas compositions and temperatures. Images A (15 nm × 15 nm) and B (7.6 nm × 7.6 nm) were acquired in 1 bar of CO at room temperature, image C(9.8 nm × 9.8 nm) at 393 K in 1.18 bar CO rich flow and images D (30 nm × 30 nm), E (9.8 nm × 9.8 nm) and F (7.6 nm × 7.6 nm) at room temperature and 1 bar of oxygen, with a low, approximately 2 mbar residual component of CO. I_t=0.2nA and V_t=0.1V.*

The survival of the Moiré pattern after the sample temperature had been raised above 100°C indicates that at the high partial pressure of CO, the

impingement rate of CO was sufficient to maintain the saturation overage of the CO overlayer, i.e. it was higher than the desorption rate of CO from the surface at that temperature. Immediately after we switched to an oxygen-rich flow the CO overlayer pattern disappeared. We interpret this as the result of the rapid removal of the adsorbed CO molecules by the reaction with the oxygen, after which the surface became oxygen covered.

Images D-F were recorded after exposing the sample to 1 bar of oxygen at 423 K, under which conditions it oxidized (see below), and subsequently cooling it down to room temperature, still in 1 bar of oxygen. To our surprise, the images no longer exhibit the characteristics of an oxide but instead they contain the Moiré pattern associated with a close-packed CO overlayer. This shows that the low residual pressure of CO (only 2mbar; to be compared with the O_2 pressure of 1 bar) is sufficient to poison the model catalyst surface at room temperature. In the light of this observation we can conclude that in order to obtain information on the structure and composition of the surface that truly applies to the situation under actual reaction conditions it is important not just to increase the pressures of the reactants into the practical regime but to also investigate the surfaces at sufficiently high temperatures, in order to avoid poisoning. Another argument to work at elevated temperatures is that the kinetic barriers for one or more of the processes may be high enough to dramatically slow down or even block the catalytic cycle. For the complete characterization of a catalytic system *temperature does matter!*

5.5.2 STM images combined with reaction kinetics

The results of a typical experiment under reaction conditions, i.e. with mixtures of CO and O_2 and at elevated temperatures, are summarized in Fig.5.3. In the upper panel a selection of images is displayed from an STM movie, showing the surface structure during the catalytic oxidation of CO on Pt (111). The lower panel depicts the partial pressures of the reactant gases CO and O_2 and the reaction product CO_2, as measured by mass spectrometry simultaneously with the STM movie. The CO_2 signal is proportional to the reaction rate. The experiment reported here started in an oxygen-rich flow of a mixture of O_2 and CO at a total pressure of 1.25 bar and a temperature of 423 K. Image G corresponds to the smooth platinum surface with large, flat terraces, separated by monatomic steps. At $t = 0$ s the CO pressure was slowly decreased and the CO_2 pressure followed this decrease until $t = 750$ s, where we observed an abrupt upward step by a factor 1.4 in CO_2 production rate (indicated by the arrow in the lower panel). The step in reaction rate occurred during the acquisition of image H. Above the dashed line in the upper part of image H we notice a dramatic change from the original, flat surface to a disorganized, rough surface. The sudden appearance of the rough structure coincided with the upward step in reaction rate. The analogy with Pt(110) and the Pd surfaces discussed in the previous chapter strongly

suggests that a surface oxide is formed, which is more reactive than the metallic surface. Image I shows the further build-up in time of rough structures that we associate with the platinum oxide. At t = 2500 s we increased the CO pressure. This resulted in an abrupt change back to a surface with flat terraces and steps with the step height of Pt(111). Initially, several Pt vacancy islands were left behind, as seen in image J that decayed with time. Following the increasing in CO pressure the reaction rate signal passed through two subsequent maxima.

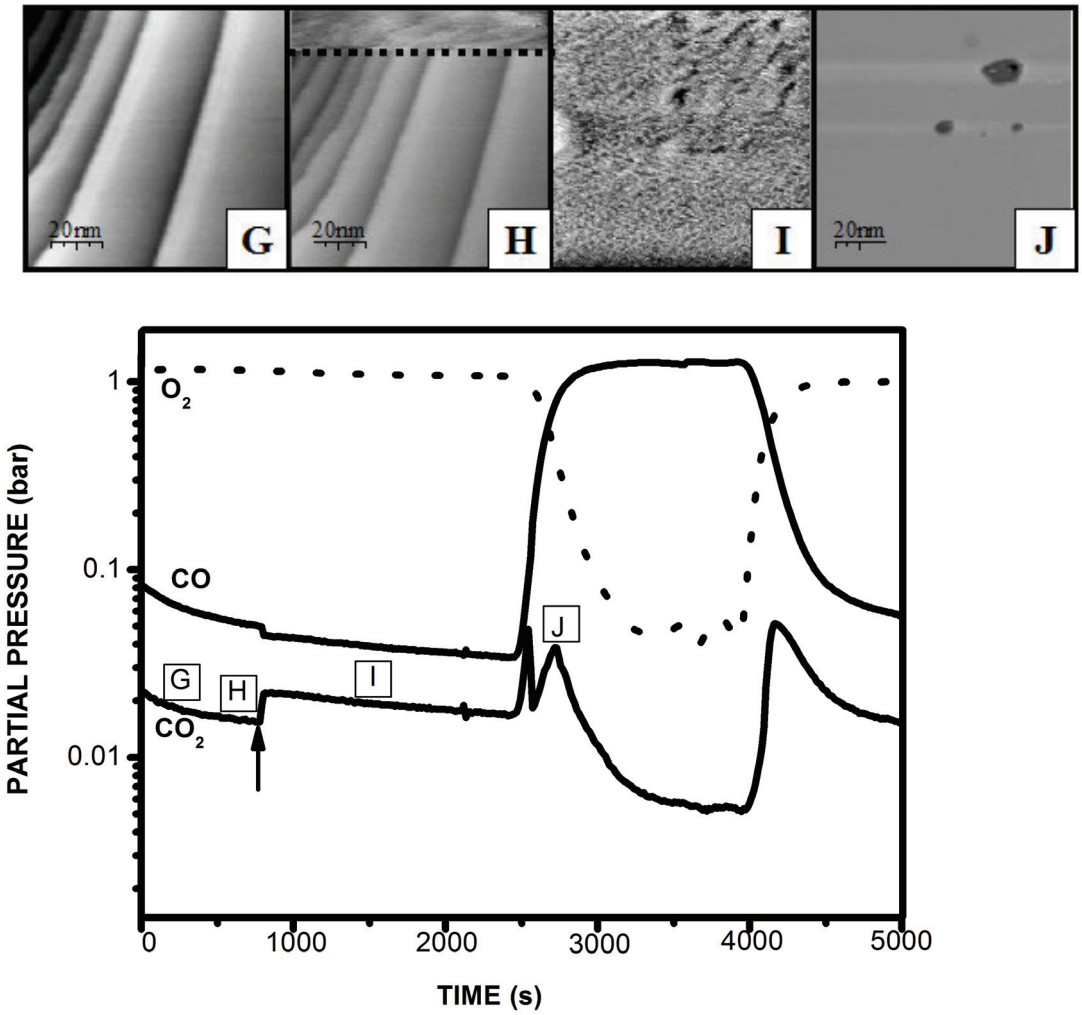

Figure 5.3: *STM images and mass spectrometer signals measured simultaneously during CO oxidation on the Pt(111) surface in a flowing mixture of O_2 and CO at a total pressure of 1.25.bar and a temperature of 423 K.*

The first one has the shape of a continuous rise in CO2 signal, starting at t = 2500 s, and a sharp downward step somewhat later. The next maximum, around t = 2750 s is broader and has no sharp features. The first peak results from the fact that the reaction rate initially follows the increase in CO partial pressure. When P_{CO} exceeds a critical value and the oxide is suddenly removed and the reactivity steps down to the lower level characteristic for

the metal surface. Indeed, this downward step coincides with the sudden change back to the flat, i.e. metallic, surface in the STM images. The second peak has the characteristics of the maximum rate in Langmuir-Hinshelwood kinetics. The presence of a peak actually implies that when the oxide surface is reduced to the metal surface, oxygen forms the dominant species adsorbed on the surface. When the partial pressure of CO is further increased, the CO coverage grows and at the maximum we have $\theta_{CO} = \theta_O = 0.5$. When P_{CO} is increased further, the reaction rate drops because carbon monoxide poisons the catalyst surface. At t = 4000 s we switched again to an oxygen-rich flow. The reaction rate increases, passes again through the maximum of Langmuir–Hinshelwood kinetics, at t = 4142 s, and then decreases again, more or less proportional to the CO pressure, as oxygen becomes the dominant surface species.

For a more detailed understanding of the above results we will go through our interpretation step-by-step and provide additional information to support our conclusions. A series of images from a different STM movie with higher resolution is shown in figure 5.4 in order to underline the changes in the surface due to exposure of high pressures reactive gases.

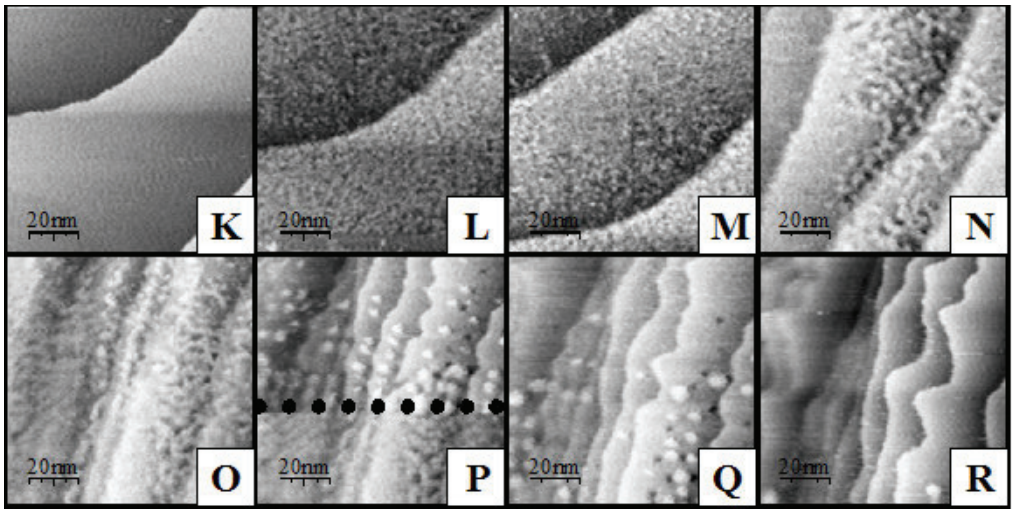

Figure 5.4: *STM images recorded in a flowing mixture of O_2 and CO at 413 K and a constant total pressure of 1.25 bar. Images K-O have been acquired in an oxygen-rich flow. Image K corresponds to the metallic Pt (100), with large flat terraces. In image L acquired immediately after image K small protrusions are visible. We assign this change of the surface to the formation of a thin platinum oxide with higher reactivity, which gradually develops cluster-type structures (images L-O and lower part of P). The upper part of image P and images Q-R correspond to the metallic surface after the oxide was removed, due to the exposure to a CO-rich flow. This removal is seen to lead to the formation of vacancy and adatom islands. In time these structures decayed and the flat surface of Pt (111) was restored. The size of the STM images is 100 nm × 100 nm. I_t=0.2 nA and V_t=0.2V.*

The metal surface before oxidation:

Image G and the lower part of image H in Figure 5.3 as well as image K in Figure 5.4 show that in the initial gas mixture, the platinum surface had the same structure as a freshly prepared clean Pt(111) surface in UHV, with flat, large terraces separated by monatomic steps (d_{step}=2.2 Å). As argued above, the observation of a maximum in the Langmuir-Hinshelwood reaction rate on the metal surface as a function of CO pressure indicates that just prior to oxidation the metal surface was covered mainly by oxygen. Since prior to oxidation there was a modest CO_2 production, resulting corresponding to a partial pressure of CO_2 of 20 mbar, also a small amount of CO must have been present on the surface in spite of the high coverage of oxygen.

The oxide evolution in time:

We assume that the oxidation of the metal surface follows the next steps:
(1) O_2 molecules reach the metal surface and O atoms are chemisorbed.
(2) As soon as the concentration of chemisorbed oxygen reaches a critical level the surface oxidizes. The oxidation itself may involve the initial formation of oxide clusters followed by lateral growth and coalescence of these.
(3) Once the layer is closed, the oxide may continue to grow in thickness, i.e. in the direction perpendicular to the surface.

For a qualitative description of the oxidation process of a surface one would need to find answers to the following fundamental questions:

(1) What is/are the oxide structure(s) and how does it depend on the oxidation parameters (temperature, pressure and gas composition)? Does it depend on the surface morphology (steps, defects, etc.)?
(2) How does the oxide thickness develop with the oxidation time (oxidation kinetics)?
(3) What is the epitaxial relation between the metal substrate and the oxide surface film?
(4) What are the rate limiting factors in the oxidation process?
(5) Is the oxide film passivating or is it catalytically active?

In our case the lack of atomic resolution makes it difficult to obtain answers to all of these questions on the basis of the STM images alone, but valuable information about the oxide could still be extracted from them.

In Figure 5.3, the upper part of image H and image I and in Fig. 5.4, images K-O and the lower part of image P (below the dashed line) show the development in time of a structure that we attribute to a form of platinum oxide. In all cases, the surface is rougher than the metallic surface, prior to

oxidation. The roughness comes in the form of pits and protrusions. As we had already seen above, this surface exhibits a higher reactivity than the metallic surface. Our conclusion that the rough, higher-reactivity surface corresponds to a surface oxide film is supported by observations with complementary techniques. Preliminary Surface X-ray Diffraction measurements by Ackermann et al. have confirmed the formation of a thin (1-2 ML) film of platinum oxide, when Pt (111) is exposed to high pressures of oxygen at high temperatures [18]. Based on these measurements, the structure of the oxide has been identified to correspond to be relaxed PtO_2, azimuthally aligned but with lattice periods that are incommensurate with the underlying Pt(111) substrate. Similar to the case of Pt(110) [19], also on Pt(111) there is an alternative, oxide-like structure that is present in a certain range of partial pressures and temperatures when both CO and O_2 are present. In this context we also recall the work by Li and co-workers, whose results on high-pressure oxidation of Pt(110) has revealed the formation and co-existence of ordered surface oxide islands with chemisorbed reconstructed (12×2)-O structure [20].

Carefully comparing the partial pressures during 50 oxidation-reduction cycles, we come to the conclusion that at fixed O_2 pressure the oxidation takes place when the CO partial pressure is lowered to a critical value. For example, at $P_{O_2} = 1.14$ bar and $T = 418$ K, this critical CO pressure is $P_{CO} = 0.022$ bar. From image H (in Fig.5.3) and upper part of image K in Fig.5.4 we have concluded that the change from a smooth, metallic surface to a rougher, oxidized surface happens within the time of one single scan line, which amounted to 1line scan/s in the present experiment. We have analysed the height profiles on the (same) middle terrace in images K and L, i.e. directly before and after oxidation, and also we have compared the Z corrugation values for the same square region in both images. Careful analysis of the individual scans lines within which the surface oxidized shows that the local height increases abruptly by 1.2 ± 0.8 Å (e.g. difference between images K and L). The large error margin reflects the fact that the change in reactivity, caused by the oxidation, also results in a stepwise change of the thermal drift, which makes it difficult to extract a reliable number for the height change. These observations are a good indication that at the beginning of the oxidation process the surface was immediately covered with a thin but rough oxide layer. Figure 5.5 repeats panel M from Fig. 5.4 and shows an enlargement of the marked, central square.

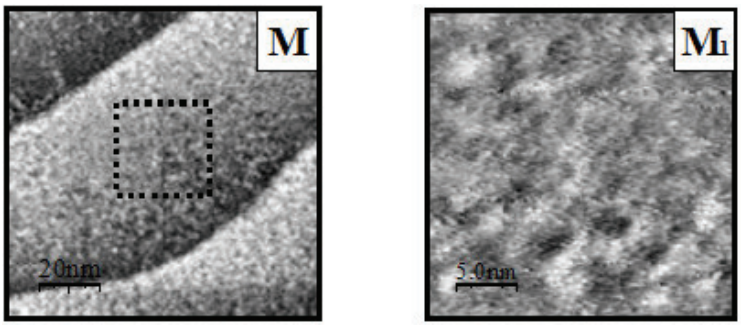

Figure 5.5: *The oxide surface immediately after oxidation (F). Image F_1 (25nm×25nm) is a zoom in on the middle terrace (dashed square) from image F (100nm×100nm). The oxide has small protrusions and pits with a typical lateral size of 2 nm and a typical height/depth of* 1 ± 0.36 *Å. I_t=0.2 nA and V_t=0.2V.*

In the next series of images (Figure 5.6) the development in time of the oxide roughness is shown from small corrugations of typically 1.25 ± 0.75 Å and short lateral length scales of typically 1.7 ± 0.2 Å to larger structures with typical dimensions of 2 ± 1 Å and 19 ± 0.5 Å in height and in width. It seems that this coarsening is not uniform over the surface and that it initiates primarily at steps, as can be seen in images M and H. The mechanism behind the preferential growth of the oxide patches might be similar to the one responsible for the formation of the denuded zones, as a result of oxygen outdiffusion during a high temperature-annealing step of a few hours, on silicon surfaces [21].

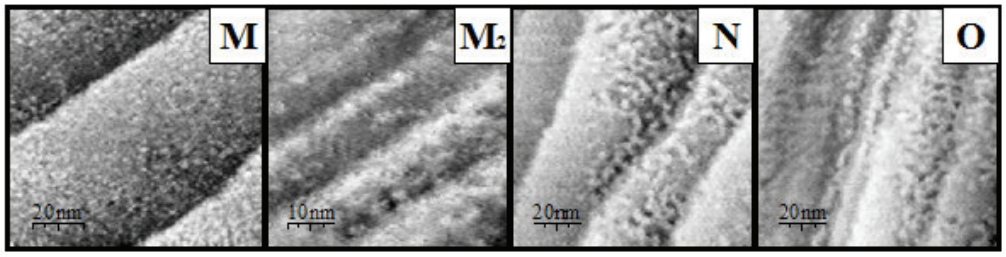

Figure 5.6: *Development of the oxide in time. After t = 138 min from the initial oxidation the features on the oxide surface have evolved from small protrusions (image M) to coarser structures (image N). This coarsening appears to initiate primarily close to steps. As the structures become coarser, the coarsening process slows down (images N, O). The size of image M is 50 nm × 50 nm, while the size of images M, N and O is 100 nm × 100 nm. I_t=0.2 nA and V_t=0.2V.*

If we zoom in on the second terrace in image N of the above series we clearly can distinguish the curved shapes of the cluster-like features and the depressions between them (figure 5.7). From the height profiles we

have found that the depths of those depressions varies between 1.45-3.2 Å, which does not correspond to the 2.2 Å atomic, step height of Pt (111).

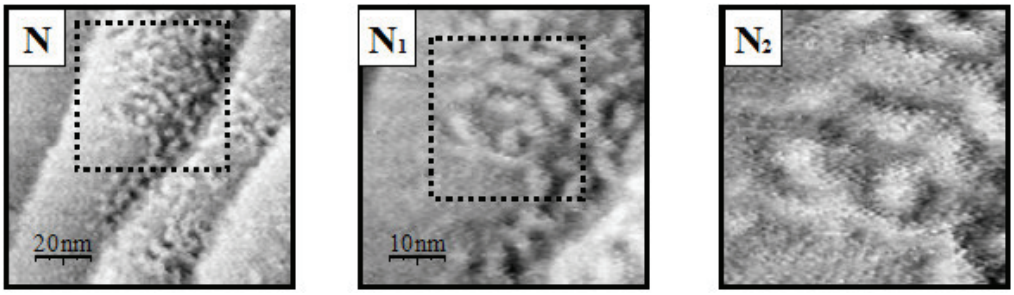

Figure 5.7: *Series of STM images (N-N_2) were we have repeatedly zoomed in, starting with the second terrace of image N of Fig. 5.6. The height profiles of these images show height variations that are all different from multiples of the step height of Pt(111). I_t=0.2 nA and V_t=0.2V. The size of the images is 100nm×100nm (N), 50nm×50nm (N_1) and 25nm×25nm (N_2).*

The metallic surface after the oxidation

When we increased the CO pressure again at t = 2520 s in Figure 5.3, the oxide was removed at a higher CO pressure of 54 mbar than the CO partial pressure of 44 mbar at which it had been formed. The metallic surface immediately after the reduction of the oxide showed a number of platinum adatom and vacancy islands (image J in Fig. 5.3 and the upper part of image P and images Q-R in Fig. 5.4). These observations are similar to those of Itaya and co-workers, who observed adatom and vacancy islands on the Pt(111) surface after cycles of an electrochemical oxidation-reduction process [22]. Figure 5.8 shows images of the metallic surface immediately after reduction of our high-pressure oxide, as observed in three different experiments performed at the same pressure (1.25 bar) but different temperatures. The imperfect hexagonal shapes of the platinum adatoms and vacancy islands reflect the triangular symmetry of Pt(111). The heights and depths of the adatom and vacancy islands correspond to one or few times (integer number) the atomic step height of Pt(111). The general trend in all experiments that we have performed is that after the removal of the oxide, if the surface is kept in a CO-rich flow, the platinum adatom and the vacancies islands disappear in time due to ripening or coalescence processes and the surface smoothens again.

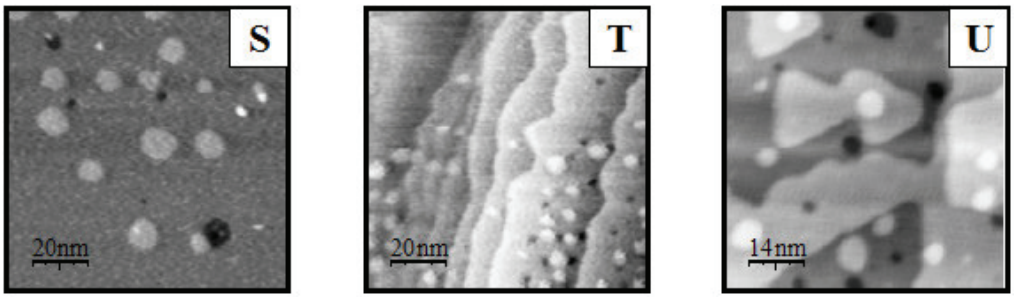

Figure 5.8: *STM images corresponding to the metallic surface, briefly after the oxide had been reduced, obtained in three different sets of measurements performed at the same pressure 1.25 bar and different temperatures. Image S (100 nm × 100 nm) was acquired at T = 373K, image T (100 nm × 100 nm) at T = 413 K and image U (70nm × 70 nm) at T = 420 K. The shape of the adatom and vacancy islands reflects the hexagonal (triangular) symmetry of Pt(111).*

5.5.3 I-V spectroscopy

In order to obtain additional information about the electronic structure of a surface one can make use of scanning tunnelling spectroscopy. We have performed scanning tunneling spectroscopy during switching experiments. The results are depicted in figure 5.9. The I-V curves corresponding to the low reactivity in the reaction kinetics were characteristic for a metallic surface (dashed lines in figure 5.9). The I-V measurements on the oxidic surface clearly showed semiconductor behaviour (continuous lines). In these measurements, the tunneling current was initially set at $I_t = 0.2$ nA at a tunnelling bias voltage of $V_t = 70$ mV for the metallic surface and $V_t = 1476$ mV for the oxide surface. The high bias voltage for the oxide surface was necessary in view of the measured band gap of the oxide. The I-V curves were measured by fixing the tip height and recording the tunnelling current as a function of tunnelling voltage over a sweep from -2 V to +2 V. Both on the metal and on the oxide surface, the I-V measurements were quite reproducible. From the I-V curves on the oxide surface we measure a band gap of 1.1 ± 0.1 eV. We have not measured systematic differences between I-V curves acquired at different locations on the oxide surface, but the I-V data were recorded only on the initial oxide, when the roughness was still small, both in height and in lateral length scale.

Unfortunately there is only limited information in the literature about the band gap of platinum surface oxide. Naegele and Plieth identified by means of the Kramers –Kronig technique a band gap of 1.4 eV for a thin (2-6 Å) oxide formed on platinum during anodic polarization [23]. In electrochemical studies on platinum electrodes band gaps varying between 0.7 and 1.3 eV have been found for different species of platinum oxides [24]. Our value of 1.1 ± 0.1 eV falls comfortably within this range of band gaps.

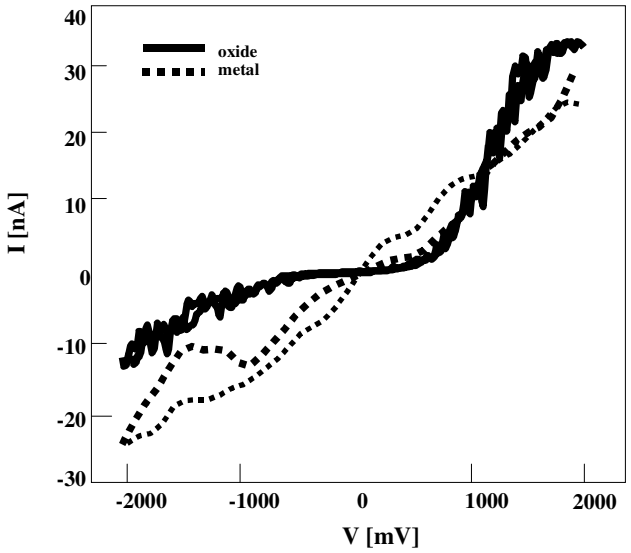

Figure 5.9: *Averaged I-V curves measured on the oxidic surface (solid line) and on the metallic surface (dotted line). The band gap measured for the oxide surface is 1.1 ± 0.1 eV.*

5.5.4 Bistability and oscillations in the reaction kinetics

As explained above, from the combined analysis of the STM images and reaction kinetics, we have concluded that during the oxidation of CO over Pt (111), a new structure is formed, which we have identified as a thin film of platinum oxide. The surface platinum oxide is formed at high partial pressure of O_2 (pressure e.g.1.12 bar) and (sufficiently) low CO partial pressure, e.g. 49 mbar in the above-mentioned experiment. In Fig. 5.10 we show that if we plot the reaction rate, measured in the form of the partial pressure of CO_2, of figure 4.3 as a function of the CO partial pressure at constant partial pressure of oxygen 1 bar), the experimental data separate into two branches. One branch corresponds to the high reactivity (oxide) and the other one to the low reactivity (the metal). Figure 5.11 summarizes the kinetics for a different set of data acquired at a total pressure of 1.25 bar and T=416 K.

Figure 5.11 (a) displays the partial pressures of the reaction product CO_2 and the partial pressure of the minor reactant CO, while the partial pressure of the major reactant O_2 was kept constant at 1.23 bar. At $t = 115$ s (indicated by the arrow) a stepwise increase in the reaction rate is recorded by the quadrupole mass spectrometer, accompanied by a step down in CO pressure. As explained earlier in this thesis, the upward step in CO_2 pressure indicates that the surface is oxidized.

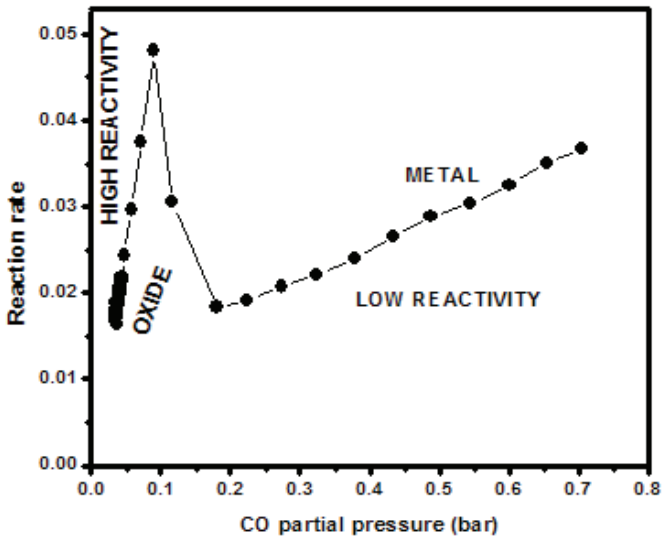

Figure 5.10: *The CO_2 pressure of figure 4.3 versus the CO pressure at a constant O_2 partial pressure of 1 bar and a temperature of 423 K. At low CO pressure the reaction rate shows two branches. The lower branch corresponds to the reaction on the metallic surface. The upper branch corresponds to the reaction on the oxide and shows a linear dependence of the CO_2-production on the CO-pressure.*

At t = 921 s, corresponding to a CO partial pressure of 0.032 bar, the system began to spontaneously oscillate. Accompanying the oscillations in CO_2 production there are clear oscillations in the CO partial pressure that have the opposite sign (i.e. P_{CO} goes down when P_{CO_2} goes up and vice versa). The period, amplitude and shape of the oscillations show a strong dependence on the CO pressure. For example, both the period and the amplitude of the oscillations decreased with decreasing the CO partial pressure. With reducing P_{CO}, the shape of the oscillations changed from the initial rectangular waveform to a 'spike' shape, with a more or less permanent high reactivity, interrupted by very brief low-reactivity excursions. Figure 5.11 (b) shows the same, oscillatory CO_2 production rate, plotted in the form of P_{CO_2} versus P_{CO}. From this graph it is clear that the reaction rate switched several times spontaneously back and forth between the familiar high (oxide) branch to the low (metallic) branch.

To some extent our measurements confirm the results of Colen and collaborators [25]. They have investigated the oxidation of carbon monoxide on Pt(111) at intermediate pressures (10^{-2} mbar of O_2). By manually varying the CO pressure the crystal has been "forced" to oscillate. Their observations showed that the reaction rate signal and the reactant CO are in antiphase and the rate oscillations occur above the bistable regime. Similar to our observations the oscillations had a rectangular waveform and a long period of several minutes.

Similarly to the behaviour of Pd(100) and vicinal Pd surface, discussed in Chapters 2 and 3, none of the models introduced previously to explain the oscillatory behaviour of CO oxidation on the platinum group metals (see Chapter 3) seems to apply to our data on Pt(111). Since Pt(111) does not have any reconstruction, the reconstruction model proposed as an explanation for the origin of the oscillations on platinum metals does not apply [26]. The faceting model is also inappropriate, since we do not observe any sign of faceting in our STM images [27]. The oxidation-reduction model proposed by Turner, Sales and Maple [28] seems to make more sense. In this model the reaction rate would oscillate between a low value, corresponding to the CO-covered metallic surface and a high value, corresponding to the mainly oxygen-covered metallic surface, via the formation of an oxide, which is considered to not be catalytically active itself. The disagreement between this model and our experimental observation is twofold. First, we do not observe the switching between two metallic versions of the surface, but only between a mainly oxygen-covered surface and an oxide. Second, the oxide is catalytically not *in*active but, in fact, it is more active than the metal.

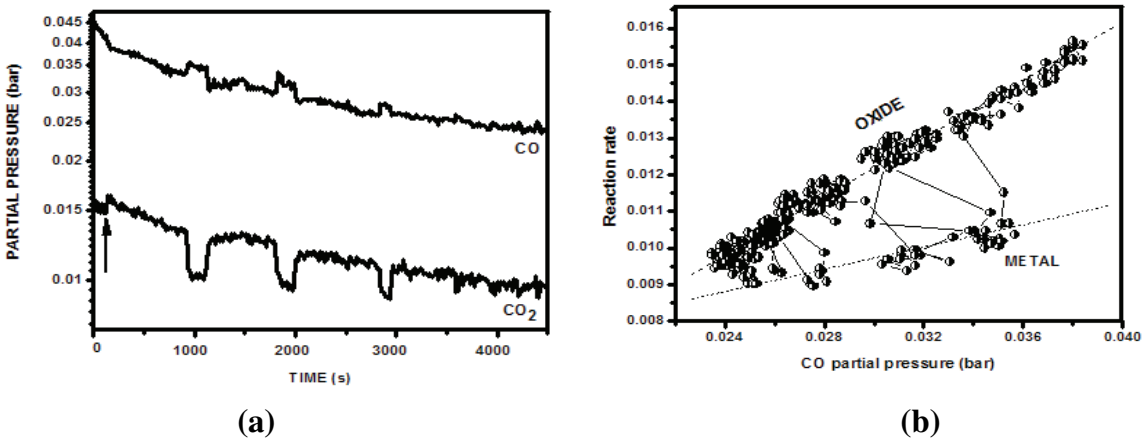

Figure 5.11: *(a) Partial pressures of CO and CO_2, during a slow, downward ramp of the CO partial pressure at T = 416 K. The O_2 pressure (not shown) was kept constant at 1.23 bar. The first metal-oxide transition occurred at t = 115 s. After this, spontaneous oscillations in the CO and CO_2-pressures were observed. (b) By re-plotting the same data in the form of P_{CO_2} versus P_{CO}, we see that the oscillations reflected the spontaneous switching between the familiar metallic and oxidic branches.*

It is important to highlight our observation that in most experiments on Pt(111) we have not observed oscillations and the hysteresis was "clockwise" (CW), meaning that the oxide was formed at a lower CO pressure than that at which it was removed. Our measurements showed that in the data sets containing oscillations, the hysteresis was always "counter

clockwise" (CCW). This is summarized in Table 4.1. The "direction" of the hysteresis might be a good indicator whether or not a catalytic system oscillates [29]. In previous studies performed in our group on CO oxidation at ambient pressure over Pt(110), spontaneous oscillations in the reaction rate have never been observed. By contrast, CO oxidation over Pd(100) showed oscillatory behaviour. The main differences between the two surfaces are: 1) the Pt(110) surface switched between an oxide and a metal surface that was mainly covered with CO, whereas Pd(100) switched between an oxide and an oxygen covered surface, similar to Pt (111) and 2) for the Pt(110) surface "clockwise" hysteresis was observed in all measurements, similar to Pt (111) for most of the experiments, while the Pd(100) surface had "anti-clockwise" hysteresis in agreement with the oscillatory data set for Pt(111). At this point, we can only speculate what parameters are responsible for the "direction" of the hysteresis. From experimental observations it has been concluded that in the case of Pd(100), the reaction-induced formation of roughness on the palladium oxide combined with a specific preference of CO for binding at the steps on the metallic surface are responsible for the "counter clockwise" orientation of the hysteresis and for the reaction oscillations on this surface (see Chapter 3). In those cases where reaction oscillations have been observed on Pt(111) the surface had been exposed to repeated cycles of oxidation-reduction, which might have created excessive roughness on the surface. Whether this can explain that oscillations sometimes but not always occur on Pt(111) remains to be investigated in more depth.

No.	P_t (bar)	T (K)	P_{CO}→M-Ox (mbar)	P_{CO} →Ox-M (mbar)	Hyst.
1	1.25	433	49	57	CW
2	1.5	433	45	110	CW
3	1.25	438	31	89	CW
4	1.25	433	47	65	CW
5	***1.25***	***408***	***47***	***28***	ACW

Table 5.1: *The direction of the hysteresis, clockwise or counter clockwise and the values of the CO pressure at which the surface switched from the metal to oxide (P_{CO}→M-Ox) and vice-versa (P_{CO}→Ox-M) are indicated for five measurements performed at different pressures and temperatures.*

5.6 Conclusions

We have studied the oxidation of CO over a Pt(111) model catalyst, using an in-situ STM combined with a flow reactor. This has allowed us to correlate the changes in the surface structure to reaction kinetics. At high CO

coverages a CO overlayer with a characteristic Moiré pattern was observed, both at room temperature and at elevated temperatures. The CO overlayer was stable under high pressures of O_2 at room temperature. Under reaction conditions two different structures have been observed, namely a (adsorbate–covered) metallic surface and an oxide. The two structures showed different reaction rates and reaction kinetics. The oxidation process has made the surface rough and the reaction has made the roughness develop further in time. The kinetics on the metallic surface followed the Langmuir-Hinshelwood mechanism, while on the oxide surface the kinetics could be explained by a Mars-Van Krevelen mechanism. Under conditions of slowly decreasing P_{CO} oscillations in the reaction rate have been observed. The mechanism responsible for making the oscillations present or absent was not fully elucidated, but our experimental observations indicate that the orientation of the hysteresis in the reaction rate might play an important role.

5.7 References

[1] http://web1.caryacademy.org
[2] http://wwww.unctad.org/infocomm/anglais/platinum/uses.htm
[3] W. J. Moore, Jr. and L. Pauling, *J. Am. Chem. Soc*. **63** (1941) 7392.
[4] E. E. Galloni and A. E. Ruffo, Jr., *J. Chem.Phys*. **9** (1941) 875.
[5] N. A. Shishakov, V.V. Andreeva and N. K. Andrushchenko, *Stronie I Mechanism Obrazovaniya Okisnykh Plenok na Metallakh, Akad. Nauk.* SSSR, Moscow 1956, Chapter 6.
[6] S. M. Ariya, M. P. Morozova, G. S. Markevich and A. A. Reikhardt, Sb. Stat. Obs. Khim. Akad. Nauk. SSSR, I (1953) 76.
[7] R. H. Busch, E. E. Galloni, J. Raskovan and A. E. Cairo, *An.Acad.Brasil.Cienc.,* **24** (1952) 185.
[8] O. Muller and R. Roy, J. *Less-Common Metals* **16** (1968) 129.
[9] R. Berry, *Surf. Sci.***76** (1978) 415.
[10] H. P. Bonzel, A. M. Franken and G. Pirug, *Surf.Sci.***104** (1981) 625.
[11] B. Lang, R. W. Joyner, and G. A. Somorjai, *Surf. Sci.* **30**(1972) 454.
[12] N. Hartmann, R. Imbihl, and W. Vogel , *Catal. Lett*. **28** ((1997) 373.
[13] G. Ertl, M. Neumann, and K. M. Streit, *Surf. Sci.*64 (1977) 394.
[14] J. A. Jensen, K. B. Reider, M. Salmeron and G. Samorjai, *Phys.Rev.Lett.*80 (1998), 1228
[15] E. K. Vestergaard, P. Thostrup, T. An, E. Laegsgaard, I. Stensgaard, B. Hammer, and F. Bessenbacher, *Phys.Rev.Lett*.88 (2002) 259601.
[16] I. Villegas and M. J. Weaver, *J. Chem. Phys.* 101 (1994) 1648.
[17] surf-prep-lab.com
[18] M. D. Ackermann et al, to be published
[19] M. D. Ackermann, T. M. Pedersen, B. L. M. Hendriksen, O. Robach, S. C. Bobaru, I. Popa, C. Quiros, H. Kim, B. Hammer, S. Ferrer, and J. W. M. Frenken *Phys. Rev. Lett*. **95** (2005) 255505
[20] W. X. Li, L. Osterlund, E. K. Vestergaard, R. T. Vang, J. Matthiesen, T. M. Pedersen, E. Laegsgaard,B. Hammer and F. Besenbacher, *Phys. Rev. Lett.* **93** (2004) 146104.
[21] G. Kissinger, J. Vanhellemont, G. Obermeir and J. Esfandyari, *Mat.Sci.and Eng*.**B73** (2000) 106
[22] K. Itaya, S. Sugawara, K. Sashikata and N. Furuya, *J. Vac. Sci. Technol.* **A 8** (1990) 515
[23] K.Naegele and W. J. Plieth, *Surf.Sci*.**50** (1975) 64.
[24] H. Angerstein-Kozlowska, B. E. Conwayand, W. B. A. Sharp, *Electroanalytical Chemistry and Interfacial Electrochemistry* **43** (1973) 9.
[25] R. E. R. Colen, J. Christoph, F.Pena,and H. H. Rotermund, *Surf. Sci.* **408** (1998) 310.
[26] S. Ladas, R.Imbihl, and G.Ertl, *Surf.Sci.***198** (1988) 42.
[27] G.Ertl, P. R. Norton and J. Rustig, *Phys.Rev.Lett.***49** (1982) 177.
[28] J. E. Turner, B. C. Sales and M. B. Maple, *Surf.Sci.***109** (1981) 591.
[29] M. Ehsasi, M. Berdau, A. Karpowicz, K. Christmann and J. H. Block, New Frontiers in Catalysis,ed.L. Guczi et al., Elsevier Science Publishers, B. V.(1993).